Role for Rab7 in maturation of late autophagic vacuoles

Stefanie Jäger[1], Cecilia Bucci[2], Isei Tanida[3], Takashi Ueno[3], Eiki Kominami[3], Paul Saftig[1] and Eeva-Liisa Eskelinen[1,*]

[1]Institute of Biochemistry, University of Kiel, Olshausenstr. 40, 24098 Kiel, Germany
[2]Dipartimento di Scienze e Tecnologie Biologiche ed Ambientali, Universita degli Studi di Lecce, 73100 Lecce, Italy
[3]Department of Biochemistry, Juntendo University School of Medicine, 2-1-1, Hongo, Bunkyo-ku, Tokyo, 113-8421, Japan
*Author for correspondence (e-mail: eleskelinen@biochem.uni-kiel.de)

Accepted 17 June 2004
Journal of Cell Science 117, 4837-4848 Published by The Company of Biologists 2004
doi:10.1242/jcs.01370

Summary

The small GTP binding protein Rab7 has a role in the late endocytic pathway and lysosome biogenesis. The role of mammalian Rab7 in autophagy is, however, unknown. We have addressed this by inhibiting Rab7 function with RNA interference and overexpression of dominant negative Rab7. We show here that Rab7 was needed for the formation of preferably perinuclear, large aggregates, where the autophagosome marker LC3 colocalised with Rab7 and late endosomal and lysosomal markers. By electron microscopy we showed that these large aggregates corresponded to autophagic vacuoles surrounding late endosomal or lysosomal vesicles. Our experiments with quantitative electron microscopy showed that Rab7 was not needed for the initial maturation of early autophagosomes to late autophagic vacuoles, but that it participated in the final maturation of late autophagic vacuoles. Finally, we showed that the recruitment of Rab7 to autophagic vacuoles was retarded in cells deficient in the lysosomal membrane proteins Lamp1 and Lamp2, which we have recently shown to accumulate late autophagic vacuoles during starvation. In conclusion, our results showed a role for Rab7 in the final maturation of late autophagic vacuoles.

Key words: Autophagy, Rab7, LC3, Lysosome, Endosome, RNA interference, LAMP deficiency, Electron microscopy

Introduction

Autophagy is a lysosomal degradation pathway for cytoplasmic material (Eskelinen, 2004; Klionsky and Emr, 2000; Mizushima et al., 2002). In mammalian cells autophagy is an important survival mechanism during short-term starvation. By degrading some nonessential components cells get nutrients for vital biosynthetic reactions. Recent results have shown that autophagy also contributes to cell homeostasis in muscle, liver and pancreas (Eskelinen et al., 2003; Tanaka et al., 2000), as well as to development, growth regulation, cancer and longevity (Liang et al., 1999; Melendez et al., 2003). After an induction signal, autophagy starts when a flat membrane cistern wraps around a portion of cytoplasm, forming a closed double-membrane-bound vacuole that contains cytoplasm (Arstila and Trump, 1968). This vacuole is called an autophagosome and it is devoid of any lysosomal proteins. Autophagosomes then undergo a stepwise maturation process including fusion events with endosomal and/or lysosomal vesicles, which leads to delivery of the cytoplasmic contents to the lysosomal compartment where it is degraded (Dunn, 1994). The degradation products are transported back to cytoplasm. The term autophagic vacuole refers to both nascent autophagosomes and autophagosomes that have fused with endosomes or lysosomes.

The first mammalian autophagy genes were identified only recently. Microtubule associated protein light chain 3 (MAP LC3, LC3) was shown to be the mammalian homologue of the yeast Atg8/Apg8/Aut7. Yeast Atg8 is needed for autophagosome formation (Lang et al., 1998) or expansion of autophagosome precursors (Abeliovich et al., 2000). LC3 peripherally localises to the inner and outer limiting membranes of autophagosomes and less so to the contents of late autophagic vacuoles (Eskelinen, 2004; Kabeya et al., 2000). Western blotting of LC3 can be used to follow the induction of autophagy during amino acid starvation, or the accumulation of autophagic vacuoles in cells treated with lysosomal enzyme inhibitors. The amount of the membrane-associated, 16 kDa LC3II increased at the same rate as the volume fraction of autophagic vacuoles in HeLa cells, while the amount of the soluble, 18 kDa LC3I decreased (Kabeya et al., 2000). It was proposed that during autophagy LC3I was processed or modified to LC3II, which then peripherally associated with the autophagosome membranes.

Most of the currently known mammalian autophagy genes including *LC3* function during the early steps of autophagy induction or autophagosome formation. On the contrary, very little is known about the proteins that regulate later steps such as maturation of autophagosomes.

Fusion events between autophagosomes and endo/lysosomes have been studied extensively in the past. Autophagosomes or autophagic vacuoles have been reported to fuse with early (Liou et al., 1997; Tooze et al., 1990) and late endosomes (Berg et al., 1998; Lucocq and Walker, 1997; Punnonen et al., 1993) as well as lysosomes (Dunn, 1990; Gordon et al., 1992; Lawrence and Brown, 1992). These results indicate that the maturation of autophagosomes in mammalian

cells is a multi-step process that includes several fusion events with vesicles originating from the endo/lysosomal compartment. The SKD1 AAA ATPase was recently shown to be necessary for autophagosome maturation (Nara et al., 2002). Early autophagosomes accumulated in cells expressing the dominant negative forms of SKD1, indicating that fewer fusion events with endo/lysosomes took place. In the yeast *Saccharomyces cerevisiae* the fusion of autophagosomes with the vacuole (yeast lysosome) was inhibited in mutants lacking Ypt7p (the yeast homologue of Rab7) (Kirisako et al., 1999), Vam3p (a syntaxin homologue) (Darsow et al., 1997), Sec18p (yeast homologue of N-ethylmaleimide sensitive factor, NSF) or Vti1p (a SNARE protein) (Ishihara et al., 2001). Although fusion of autophagosomes with the vacuole was inhibited in yeast strains deficient in these proteins, it is not known whether any of these proteins, including Rab7, localises in yeast autophagosomes. Only one of these proteins has been investigated in the context of mammalian autophagy. Fusion of mammalian autophagosomes with multivesicular endosomes was partially retarded in hepatocytes isolated from mice deficient in Vti1b (Atlashkin et al., 2003), suggesting that this protein might participate in the autophagosome fusion processes also in mammalian cells. However, the roles of Rab7 (Ypt7), syntaxins and NSF in mammalian autophagy are unknown.

Rab7 is a small GTP binding protein that has functions in late endosomal transport (Press et al., 1998; Vitelli et al., 1997) and lysosome biogenesis (Bucci et al., 2000). It is generally used as a late endosome marker protein (Bottger et al., 1996). Rab proteins peripherally associate with membranes via a geranylgeranyl lipid tail. The GTP-bound form of Rab proteins is generally thought to interact with the effector proteins and thus mediate the functions of the Rab proteins. The GDP-bound form is thought to be inactive and when overexpressed, it acts as a dominant negative inhibitor (Somsel Rodman and Wandinger-Ness, 2000; Stenmark and Olkkonen, 2001). In this paper we addressed the role of Rab7 in autophagosome and autophagic vacuole maturation in HeLa cells using Rab7 RNA interference (RNAi) and overexpression of dominant negative Rab7.

Materials and Methods

Cell lines

HeLa cells and mouse embryonic fibroblasts were cultured in DMEM 10% fetal calf serum and penicillin-streptomycin at 5% CO_2. To induce autophagy the cells were incubated in serum and amino acid free medium (EBSS, Invitrogen, Karlsruhe, Germany) for 1-4 hours.

Antibodies and constructs

Rabbits were immunised with recombinant full-length GST::LC3 expressed in *Escherichia coli*. The antibodies were purified by affinity chromatography on a GST-LC3-Sepharose column. Then anti-GST reactivity was removed by passing the antibodies through a GST-Sepharose column. The resulting anti-LC3 did not cross-react with the other Apg8/Atg8 homologues, GATE-16 or GABARAP. In western blots of HeLa cell extracts, the anti-LC3 recognised three bands approximately at 30, 18 and 16 kDa, corresponding to the precursors LC3, LC3I and LC3II, respectively. In addition, the following primary antibodies were used: rabbit anti-Rab7 (Suzanne Pfeffer, Stanford University, CA), chicken anti-Rab7 (Angela Wandinger-Ness, University of New Mexico, NM), mouse anti-Rab5 (Stressgen Biotechnologies, Victoria, Canada), mouse anti-LBPA (lysobisphosphatidic acid) (Kobayashi et al., 1998), rabbit anti-GFP (green fluorescent protein) (Research Diagnostics, Flanders, NJ) and mouse anti-human LAMP1 (lysosome associated membrane protein) (Developmental Studies Hybridoma Bank, Iowa City, IA). In western blots both chicken and rabbit anti-Rab7 recognised one ~22 kDa band in extracts from nontransfected cells, and two bands at ~22 and ~45 kDa in extracts from GFP-Rab7 expressing cells (not shown), indicating that the antibodies were specific for Rab7. N-terminally GFP-tagged constructs for wild type, constitutively active (Rab7Q67L) and dominant negative (Rab7T22N) Rab7, in pEGFP-C1 plasmid (Clontech, Palo Alto, CA), have been described and characterised before (Bucci et al., 2000). The identity of the constructs was verified by sequencing.

Transfections

GFP-Rab7 constructs and RNAi vectors were transfected using Fugene 6 (Roche, Mannheim, Germany) for immunofluorescence microscopy, or Cell Line Nucleofector Kit R (Amaxa GmbH, Cologne, Germany) for western blotting and electron microscopy, according to instructions given by the manufacturer.

RNAi

The pSUPER vector (Brummelkamp et al., 2002) was used to produce small interfering RNA molecules in transiently transfected HeLa cells. A 64 nucleotide long insert containing a Rab7-specific 19 nucleotide dsRNA hairpin coding sequence (5′cggttccagtctctcggtg 3′ corresponding to human Rab7 cDNA 205-223) was generated by annealing two complementary oligoribonucleotides containing the Rab7 sequence as an inverted repeat, separated by a 9 nucleotide long hairpin region. The hybridised oligonucleotides were inserted to the *Bg1*II/*Hin*dIII site of the pSUPER plasmid. Cells were transiently transfected by nucleofection with the plasmid, or the empty pSUPER as a control, and used for experiments 3 days later.

Western blotting

Cells were extracted using phosphate buffered saline (PBS) containing 2% NP-40, 0.2% SDS and a proteinase inhibitor cocktail (Roche, Mannheim, Germany). After SDS-polyacrylamide gel electrophoresis, the proteins were transferred to PVDF membranes using a semi-dry blotting system. Transfer efficiency was checked with Ponceau staining. The blots were blocked in Tris-buffered saline (TBS) containing 5% skimmed milk powder. Horseradish peroxidase-conjugated donkey anti-rabbit or anti-mouse IgG, or donkey anti-chicken IgY (Santa Cruz Biotechnology, Santa Cruz, CA) were used as secondary antibodies. The signals were detected using ECL Plus Western Blot Detection System (Amersham, Little Chalfont, UK).

Immunofluorescence

Cells were grown on glass coverslips. After experimental procedures, the cells were washed with PBS and fixed in cold methanol (–20°C, 5 minutes) or in 4% paraformaldehyde in PBS for 30 minutes. After the latter fixation the cells were treated with 0.12% glycine and permeabilised in 0.2% saponin in PBS. Goat anti-rabbit IgG and goat anti-mouse IgG coupled to Alexa Fluor 350, 488 or 594 (Molecular Probes, Eugene, Oregon), or goat anti chicken IgY coupled to Texas Red (Santa Cruz), were used as secondary antibodies. The samples were embedded in Mowiol containing DABCO and examined with a Zeiss Axioskop 200M using Plan Apochromat 63X/1.4 Oil objective. Optical sections were generated using the ApoTome device and photographed with Axiocam MRm Rev. 2(D) camera and AxioVision Software Rel. 4.1 (Zeiss, Göttingen, Germany). Images were prepared for presentation using Adobe Photoshop 6.0.

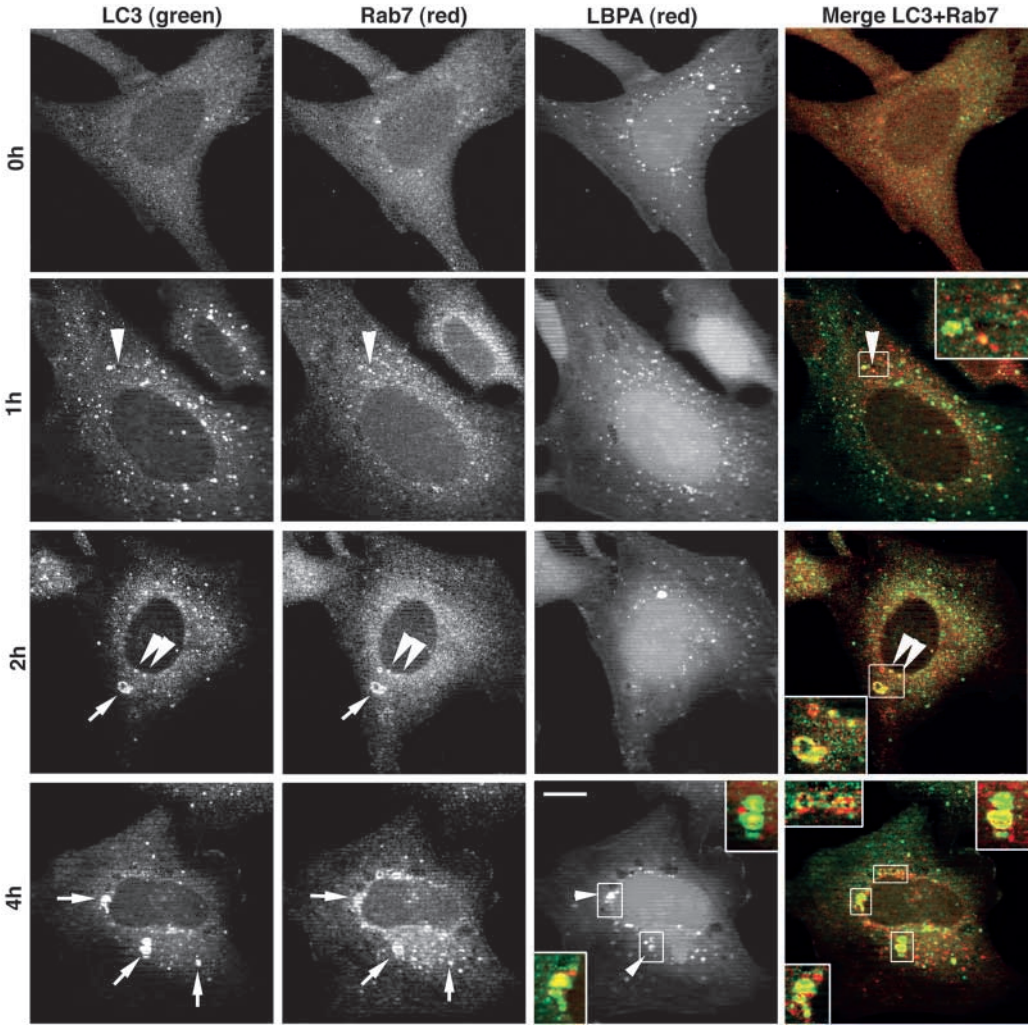

Fig. 1. LC3 and Rab7 distributions changed during amino acid starvation. Triple immunofluorescence staining of LC3, Rab7 and lysobisphosphatidic acid (LBPA) in HeLa cells. The cells were grown on coverslips and either fixed without treatment (0 h) or incubated in serum and amino acid free medium for 1 to 4 hours as indicated on the left. The cells were fixed with 4% paraformaldehyde and permeabilised with saponin. Optical sections are shown. Overlay of LC3 (green) and Rab7 (red) is shown in the right column. Arrows and inserts in the 2 h and 4 h rows indicate large LC3-positive structures, which started to appear after 2 hours starvation. These structures were also positive for Rab7, as indicated by the arrows in the Rab7 column and yellow colour in the merge column. At later time points, LBPA was also present in these structures, as indicated by small arrowheads, and yellow colour in the inserts, in the LBPA column (LC3 is green, LBPA red). LC3 and Rab7 also colocalised in small vesicles that probably represent newly formed autophagosomes (large arrowheads in 1 h and 2 h cells). Bar, 10 μm.

Electron microscopy and quantitation

For Epon embedding, cells were fixed in 2% glutaraldehyde in 0.1 M Hepes buffer pH 7.4, scraped off the culture dish, pelleted and embedded in Agar100 resin. Autophagic vacuoles were counted under the Zeiss EM 900 electron microscope at 12,000× magnification using grid squares as sampling units. All autophagic vacuoles found in the grid square were counted, and the cell area in the square was estimated by point counting using a photograph of the whole square, taken at 400× magnification. Three to five grid squares were counted from each sample. For immunoelectron microscopy, nontransfected cells, cells expressing GFP-Rab7 constructs or cells expressing GFP only were fixed using 4% paraformaldehyde, 0.1% glutaraldehyde in 0.1 M Hepes buffer for 1 hour at room temperature, scraped off the culture dish, embedded in 12% gelatine, infiltrated in polyvinylpyrrolidone-sucrose and frozen to sample holders. Thin sections were cut at –100°C, picked up with sucrose-methyl cellulose and mounted on Pioloform-carbon coated grids. The grids were immunolabelled using rabbit anti-GFP, rabbit anti-LC3 or mouse anti-Lamp1, followed by goat anti-rabbit or anti-mouse IgG conjugated to 10 nm or 5 nm gold particles (British BioCell, Cardiff, UK). For double labellings, two primary antibodies, originating from different species, were mixed. Finally grids were embedded in methyl cellulose-uranyl acetate and dried. Labelling densities of LC3 and GFP-Rab7 were estimated by counting the number of gold per vacuole under the microscope (20,000× magnification) and estimating the size of the autophagic vacuole profiles by point counting, using photographs taken at 7000× magnification.

Subcellular fractionation

Autophagic vacuoles and lysosomes were isolated from the livers of rats administered with leupeptin/E64c or dextran, respectively, as described previously (Kabeya et al., 2000; Ueno et al., 1991). The isolated autophagic vacuoles and lysosomes were subjected to hypotonic rupture and membranes were subsequently separated by discontinuous sucrose-gradient centrifugation (Ueno et al., 1991).

Results

LC3-positive autophagosomes form randomly in the cytoplasm and then form large aggregates mainly in the perinuclear region

The recent discovery of the autophagic vacuole marker protein LC3 has made it possible to follow autophagy induction by immunofluorescence microscopy. To be able to use this approach we first tested by immunoelectron microscopy the selectivity of LC3 labelling in HeLa cells. Autophagic vacuoles were classified to early – containing morphologically intact cytoplasm – and late – containing partially degraded cytoplasm (Eskelinen, 2004; Tanaka et al., 2000) (Fig. 2). Approximately 59% and 29% of early and late autophagic vacuole profiles, respectively, were positive for LC3 (contained three or more gold particles for LC3). The labelling density was 9.42±1.30 gold particles/μm^2 in early vacuoles, and 4.42±0.76 gold

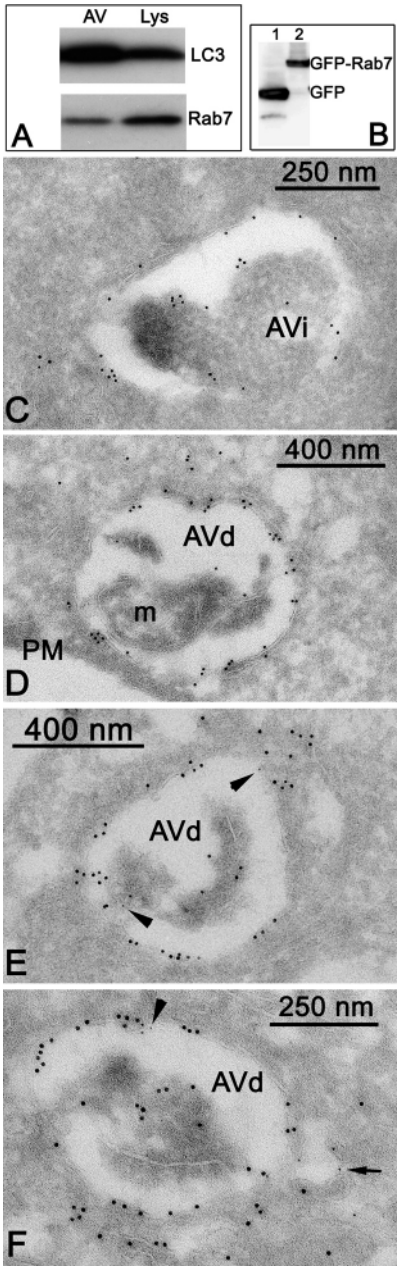

Fig. 2. Rab7 localised in the membranes of autophagic vacuoles. (A) Subcellular fractionation of rat liver. Rab7 was detected by western blotting in both autophagic vacuolar membranes and lysosomal/late endosomal membranes. The characterisation of the fractions has previously been published (Kabeya et al., 2000). LC3II only is shown, as no LC3I was detected in the membrane fractions. (B-F) Localisation of GFP-Rab7 by immunoelectron microscopy. HeLa cells were transfected with pEGFP-Rab7 and grown for 1 day. The cells were starved of amino acids for 2 hours and prepared for immunogold labelling with anti-GFP (10 nm gold) and anti-Lamp1 (5 nm gold) antibodies. (B) Western blotting was used to show that all GFP was still connected to Rab7 in these conditions. Lane 1, cells transfected with GFP, and lane 2, cells transfected with GFP-Rab7. Early autophagic vacuoles (AVi) showed labelling for GFP-Rab7 in the outer and inner membranes (C). (D-F) Late autophagic vacuoles (AVd) with their limiting membranes labelled for GFP-Rab7. Some GFP-Rab7 was also present in the contents, in agreement with the association of GFP-Rab7 with both the outer and inner limiting membranes of the early vacuoles (C). Some AVd were also weakly labelled for Lamp1 (E and F, arrowheads), or Lamp1 was present in vesicles close to them (F, arrow). The AVd in D contains a partially degraded mitochondrion (m). PM, plasma membrane.

particles/μm^2 and late vacuoles (P=0.0014, t-test). Thus, immunofluorescence of endogenous LC3 was likely to reveal preferably early, but also a subpopulation of late, autophagic vacuoles. Labelling of late autophagic vacuoles with anti-LC3 was in agreement with earlier studies showing that some LC3 was targeted to the autophagosome lumen (Kabeya et al., 2000). This LC3 is detectable with antibodies until it is degraded by the incoming lysosomal hydrolases.

To investigate the location of autophagic vacuoles in cells, we next studied the distribution of LC3-positive autophagosomes by immunofluorescence microscopy. HeLa cells were starved of serum and amino acids for different time periods, fixed and stained with antibodies against LC3 and Rab7. Lysobisphosphatidic acid (LBPA), a late endosomal/lysosomal lipid (Kobayashi et al., 1998; Möbius et al., 2003) was also labelled to check the localisation of an additional endo/lysosomal contents marker, which will be discussed later. The specificity of anti-LC3 and anti-Rab7 was shown by western blotting as described in Materials and Methods. In nonstarved cells, LC3 staining (left column in Fig. 1) was mostly diffuse (Fig. 1, 0 h). After 1 hour starvation bright vesicular structures appeared randomly around the cytoplasm (Fig. 1, 1 h). After 2 hours starvation larger, mainly perinuclear, ring-like structures became visible in addition to the smaller bright vesicles (Fig. 1, 2 h, arrow). The smaller bright vesicles seemed to decrease in number while the larger structures appeared. After 4 hours starvation the majority of the small bright vesicles had disappeared but the large, mainly perinuclear structures were visible in the majority of cells (Fig. 1, 4 h). Surprisingly, Rab7 localisation also changed during amino acid starvation (second column in Fig. 1). While in nonstarved cells only few faint vesicular structures were visible in the majority of cells (Fig. 1, 0 h), bright vesicles appeared after 1 hour starvation and became more evident with increasing time of starvation. After 2 hours starvation larger Rab7-positive structures also became evident (Fig. 1, 2 h, arrow). Rab7 and LC3 colocalised both in the small dots (large arrowheads in Fig. 1) and especially in the large, mainly perinuclear structures (arrows in Fig. 1). Colocalisation of LC3 and Rab7 is seen as yellow in the merge column of Fig. 1. Immunofluorescence localisation of endogenous Rab7 is known to be difficult because the membrane association, mediated by the geranylgeranyl lipid tail, is easily lost during sample preparation. The colocalisation of Rab7 with LC3 in Fig. 1 is thus likely to represent an underestimation of the localisation of Rab7 in LC3-positive autophagic vacuoles.

To confirm the localisation of Rab7 in autophagic compartments we performed subcellular fractionation and immunoelectron microscopy. We have previously published the characterisation of the autophagic vacuolar and lysosomal/late endosomal membrane fractions used in this study (Kabeya et al., 2000). Using these fractions, we showed by western blotting that both autophagic vacuole and lysosome/late endosome membrane fractions contained Rab7 (Fig. 2A). This result was in agreement with our

immunofluorescence analysis (Fig. 1) and earlier reports (Bucci et al., 2000). For immunoelectron microscopic localisation of Rab7, we used transiently transfected GFP-Rab7. This was necessary for immunoelectron microscopy of Rab7 as the endogenous expression level was too low for detection. We have shown previously that the protein encoded by the GFP-Rab7 construct used in this study was functional (Bucci et al., 2000). Western blotting of cells expressing GFP-Rab7 showed that after a 2 hour starvation, all GFP was still bound to Rab7 and very little free GFP was detected (Fig. 2B, lane 2). Cells starved of serum and amino acids for 2 hours were fixed and prepared for immunogold labelling with anti-GFP antibodies. Autophagic vacuoles were identified morphologically as membrane-bound vesicles containing intact or partially degraded cytoplasmic material. The inner and outer limiting membranes of autophagosomes were heavily labelled for GFP-Rab7 (Fig. 2C). Labelling for GFP-Rab7 was also observed in the limiting membranes of later autophagic vacuoles (AVd, Fig. 2D-F) containing partially degraded cytoplasm. The sections were scanned to quantitate the proportion of autophagic vacuoles positive for GFP-Rab7. According to the number of gold particles associated with the limiting membrane, the vacuoles were scored as unlabelled (0-2 gold particles), moderately labelled (3-9 gold particles) or heavily labelled (10 or more gold particles). For early vacuoles, 24% were moderately labelled and 57% were heavily labelled, giving a total of 81% of AVi positive for GFP-Rab7. For late vacuoles, 23% were moderately labelled and 72% were heavily labelled, giving a total of 95% of AVd positive for Rab7. Thus, the majority of both AVi and AVd were positive for GFP-Rab7, but the labelling intensity increased during vacuole maturation. Some GFP-Rab7 labelling was also present in the contents of autophagic vacuoles (Fig. 2C-F) suggesting that similar to LC3, some GFP-Rab7 was trapped inside autophagosomes. This intra-autophagosomal GFP-Rab7, however, represented only a small proportion of the total autophagosomal GFP-Rab7. Cells expressing GFP only were used to control the specificity of Rab7 labelling. In these cells anti-GFP labelling was seen in the cytoplasm but it was not associated with any membrane structures (not shown). These results (Figs 1-2) indicate that both endogenous and overexpressed Rab7 localised in the limiting membranes of autophagic vacuoles, which suggested that Rab7 may have a role in autophagic vacuole maturation.

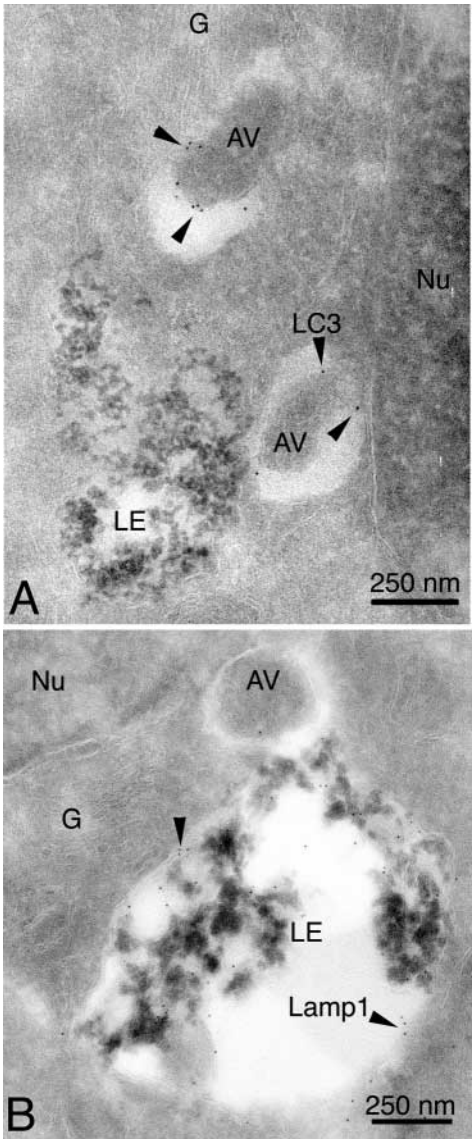

Fig. 3. Autophagic vacuoles were frequently detected in the perinuclear area close to the Golgi apparatus. HeLa cells were starved for 2 hours to induce autophagy and prepared for immunogold labelling of LC3 (A) or Lamp1 (B) followed by a secondary antibody coupled to 5 nm gold (arrowheads). Autophagic vacuoles (AV) were frequently observed to accumulate close to the nucleus (Nu) and the Golgi stack (G), where endo/lysosomal vacuoles (LE) were also present. Some autophagic vacuoles were observed to fuse with the Lamp1-positive endo/lysosomal vacuoles (B).

Rab7 was delivered to autophagosomes before LBPA or Lamp1

To get insight into the kinetics of autophagosome maturation, we examined LBPA and Lamp1 labelling of autophagic vacuoles. LBPA staining was used to study fusion events between autophagic vacuoles and endo/lysosomes (Fig. 1, third column). Colocalisation of LC3 and LBPA was mainly observed in the large perinuclear structures, which also contained Rab7 (Fig. 1, 4 h, small arrowheads and inserts).

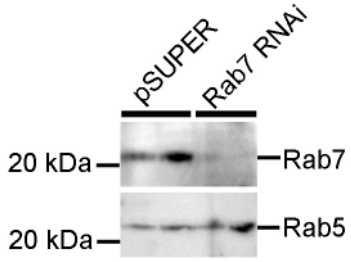

Fig. 4. Effect of transfection with the Rab7 RNAi construct on Rab7 and Rab5 levels. HeLa cells were transiently transfected with empty pSUPER or pSUPER containing the Rab7 RNAi insert. Two parallel dishes were prepared for each construct. After 3 days the cells were prepared for western blotting with anti-Rab7 and anti-Rab5. Equal amounts of protein were loaded in each lane. Notice that Rab7 was heavily downregulated, whereas Rab5 was not affected.

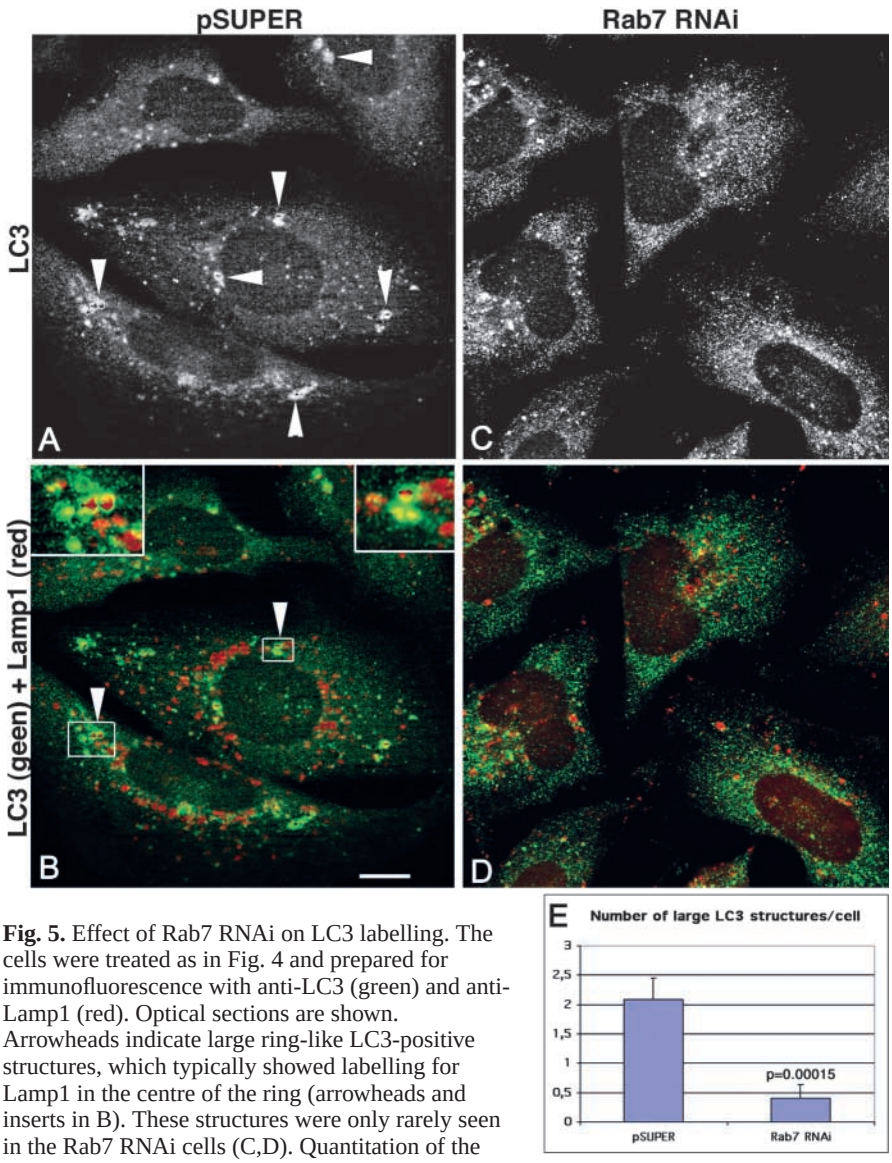

Fig. 5. Effect of Rab7 RNAi on LC3 labelling. The cells were treated as in Fig. 4 and prepared for immunofluorescence with anti-LC3 (green) and anti-Lamp1 (red). Optical sections are shown. Arrowheads indicate large ring-like LC3-positive structures, which typically showed labelling for Lamp1 in the centre of the ring (arrowheads and inserts in B). These structures were only rarely seen in the Rab7 RNAi cells (C,D). Quantitation of the large LC3- and Lamp1-positive structures per cell is shown in E. Statistical significance was estimated using *t*-test. Bar, 10 μm.

During starvation colocalisation of LC3 with Rab7 was observed at earlier time points (after 1 hour starvation) than with LBPA (after 2-4 hours starvation). Double labelling of GFP-Rab7 and the lysosomal membrane protein Lamp1 was investigated using immunoelectron microscopy (Fig. 2D-F). We have previously shown that labelling for Lamp1 was weak in early autophagic vacuoles, but increased during maturation into late vacuoles (Eskelinen et al., 2002b; Tanaka et al., 2000). In agreement with these results, no labelling for Lamp1 was observed in early autophagic vacuoles in HeLa cells. However, weak but consistent labelling for Lamp1 was observed in late autophagic vacuoles positive for GFP-Rab7 (Fig. 2E,F, arrowheads), and in vesicles close to these autophagic vacuoles (Fig. 2F, arrow). The latter may represent vesicles that deliver Lamp1 to autophagic vacuoles. Together, these results suggested that Rab7 was delivered to autophagosomes before fusion with LBPA- or Lamp1-positive endo/lysosomal vesicles.

The large ring-shaped LC3 structures consisted of several autophagic vacuoles surrounding endo/lysosomal vesicles

Taken together, our results suggested that autophagosomes formed randomly in the cytoplasm and then formed larger aggregates in or close to the perinuclear region. During this process autophagosomes acquired Rab7. Autophagic vacuoles formed larger structures by aggregating and/or fusing with other autophagosomes and/or endosomal and lysosomal vesicles. To get more insight into the nature of the large LC3-positive structures (arrows in Fig. 1) we performed immunoelectron microscopy. Because transfection may cause aggregation of proteins or organelles to the perinuclear region, we used nontransfected cells for these experiments, similar to the immunofluorescence analysis shown in Fig. 1. In HeLa cells starved for 2 hours, LC3-positive autophagic vacuoles were frequently observed to accumulate close to the nucleus and Golgi apparatus, where late endosomes or lysosomes were also observed (Fig. 3A,B). Fusion profiles of autophagic vacuoles with Lamp1-positive endo/lysosomes were also detected (Fig. 3B). The large, often ring-like LC3- and Rab7-positive structures observed by immunofluorescence and optical sectioning after 2 and 4 hours starvation (arrows in Fig. 1, see also Fig. 5B) may thus represent aggregates of autophagic vacuoles, possibly surrounding endo/lysosomal vesicles to deliver their cytoplasmic contents for degradation, as suggested by Fig. 3B. However, because of the limited thickness of electron microscopy sections (maximum 100 nm), it was not possible to catch the entire ring-like structure in one thin section.

Downregulation of Rab7 expression with RNAi abolished the formation of large LC3 structures and retarded the maturation of autophagic vacuoles

Next we wanted to address whether Rab7 had a function in autophagic vacuoles. To do this we tested whether downregulation of Rab7 with RNAi had an effect on autophagic vacuole maturation. We constructed a Rab7 RNAi expression vector using pSUPER (Brummelkamp et al., 2002). HeLa cells were transiently transfected and Rab7 expression was followed by western blotting with Rab7 antibodies. Rab5 was blotted as a control. Three days after transfection the expression of Rab7 was at its lowest (about 5% of control cell level, Fig. 4, Fig. 6A), after which the Rab7 levels started to increase slowly (not shown). The expression level of Rab5 did not change (Fig. 4), indicating that the effect of our construct

was specific for Rab7. Downregulation of Rab7 indicated that the transient transfection was very efficient and that the RNAi vector was functional.

We first tested the effect of Rab7 RNAi on LC3 immunofluorescence staining pattern. HeLa cells were transiently transfected with empty pSUPER or pSUPER Rab7 RNAi vector, incubated for 3 days and starved for 2 hours to induce autophagy. LC3 and Lamp1 were detected by double immunofluorescence staining. Large LC3- and Lamp1-positive structures were observed in 70% of cells treated with empty pSUPER (Fig. 5A,B, arrowheads), while these structures were only found in 13% of the Rab7 RNAi cells (Fig. 5C,D). The average number per cell of these large LC3 structures was 5.1 times higher in pSUPER cells than in Rab7 RNAi cells (Fig. 5E, P=0.00015, t-test). Although the large LC3 structures were seldom observed in the Rab7 RNAi cells, smaller LC3-positive vesicles were present (Fig. 5C). Similar smaller LC3 vesicles were also detected in the pSUPER cells in addition to the large LC3 structures (Fig. 5A).

Interestingly, in cells transfected with the empty pSUPER vector, Lamp1 staining was typically observed in the centre of the ring-shaped LC3 structures (Fig. 5B, arrowheads and inserts). This staining pattern suggested that many LC3-positive autophagic vacuoles had accumulated around Lamp1-positive endo/lysosomes, in agreement with the electron microscopical findings (Fig. 3B). While the majority of the large LC3-positive structures was observed in the perinuclear region, a few were also detected further away from the nucleus (Fig. 5A,B).

We next investigated the effect of Rab7 RNAi on LC3I and LC3II levels in western blots. Accumulation of the membrane-bound LC3II has been suggested to correlate with accumulation of autophagic vacuoles (Kabeya et al., 2000). However, in cases where mainly late autophagic vacuoles accumulated, LC3II levels were not different, or differed only slightly, from controls (Eskelinen et al., 2004). HeLa cells were transfected with pSUPER or pSUPER Rab7 RNAi and grown for 3 days. Three parallel dishes were starved of amino acids for 2 hours, and another three dishes were first starved for 2 hours and then switched back to full culture medium with fetal calf serum for 2 hours to allow maturation of the autophagic vacuoles formed during starvation (Eskelinen et al., 2002a). Similar amounts of LC3II were detected in pSUPER and Rab7 RNAi cells after the 2 hour starvation. After 2 hours starvation and 2 hours chase, however, the amount of LC3II was approximately 1.3 times higher in the RNAi cells when compared with the cells transfected with the empty pSUPER (Fig. 6A). Because the levels of LC3II were only slightly affected, accumulation of early autophagic vacuoles was not likely in the Rab7 RNAi cells. If any, late autophagic vacuoles may have accumulated in these cells. The higher amount of LC3II in the RNAi cells after the 2 hour chase suggested that the maturation of late autophagic vacuoles, and degradation of their contents including the LC3II trapped inside the vacuoles, were retarded.

To confirm the immunofluorescence and western blotting results we also performed electron microscopy. We have previously shown that retarded maturation of late autophagic vacuoles is detected as an increased accumulation of these vacuoles in quantitative electron microscopy (Eskelinen et al., 2002a; Tanaka et al., 2000). We used this approach to estimate

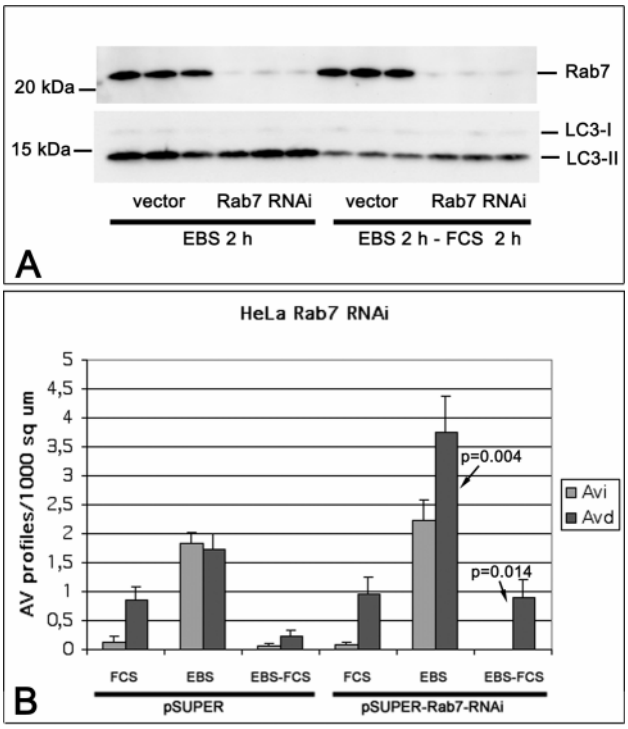

Fig. 6. Downregulation of Rab7 expression with RNAi caused accumulation of late autophagic vacuoles. HeLa cells were transfected with empty pSUPER or pSUPER Rab7 RNAi and grown for 3 days. Three parallel dished were kept in full culture medium (FCS), another three dishes were starved of amino acids for 2 hours (EBS), and another three dishes were first starved of amino acids for 2 hours and then shifted back to full medium for 2 hours (EBS – FCS). (A) Expression levels of Rab7 and LC3 were controlled by western blotting. Equal amounts of cell extract (40 μg) were loaded in each lane, and Ponceau staining was used to confirm equal transfer of proteins to each lane on the PVDF membrane (not shown). (B) Accumulation of early (Avi) and late (Avd) autophagic vacuoles was estimated by quantitative electron microscopy. The P values indicate statistical significance of the difference between the Rab7 RNAi and the pSUPER sample (t-test). Error bars indicate s.e.m.

the amounts of autophagic vacuoles in the pSUPER and Rab7 RNAi cells treated identically to the cells used for immunofluorescence and western blotting. In pSUPER cells, we observed a starvation-induced increase in the amount of early and late autophagic vacuoles as expected (Fig. 6B). During the 2 hour chase in full medium these autophagic vacuoles almost completely disappeared, indicating that the cytoplasmic contents were degraded. In the Rab7 RNAi cells after 2 hours starvation, the amount of early vacuoles was only slightly larger than in the pSUPER cells (not statistically significant), while the amount of late vacuoles (Avd) was twice as large as in the pSUPER cells (P=0.004, Mann-Whitney U-test). The accumulation of late autophagic vacuoles indicated that the conversion of Avi to Avd proceeded normally, but the maturation of Avd was retarded. A significant portion of the Avds was still present in the RNAi cells after the 2 hour chase in full medium (P=0.014). The latter observation is in agreement with the results of the LC3 western blot showing

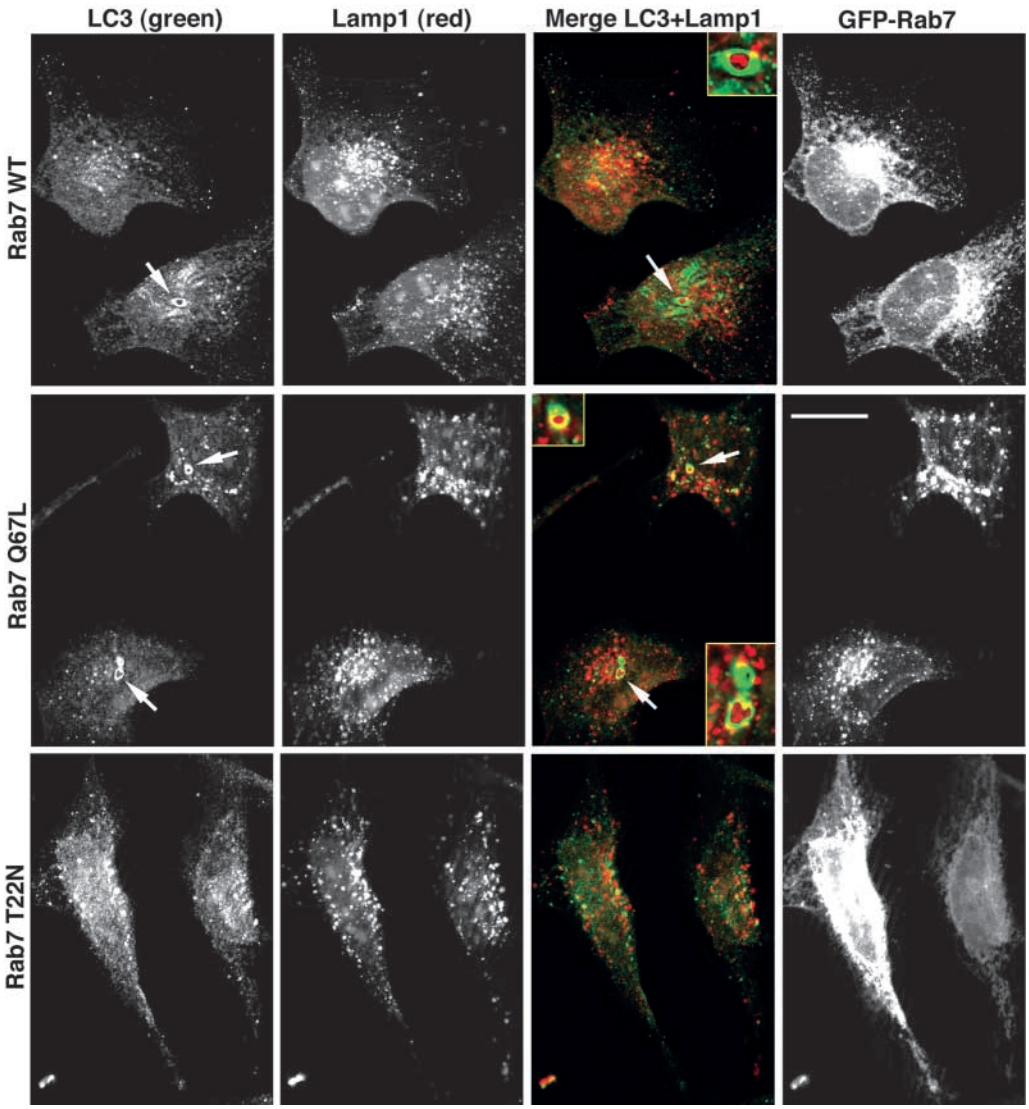

Fig. 7. Effect of Rab7 constructs on localisation of endogenous LC3 in HeLa cells. The cells were transiently transfected with pEGFP-Rab7 wild-type (WT), Q67L (constitutively active) or T22N (dominant negative) as indicated on the left, and grown for 1 day. The cells were starved of serum and amino acids for 2 hours, fixed in cold methanol, and LC3 and Lamp1 were stained by immunofluorescence. Optical sections are shown. Overlay of LC3 (green) and Lamp1 (red) is shown in the third column. The fourth column shows GFP fluorescence from the Rab7 constructs. Notice the large ring-shaped LC3-positive structures in Rab7 WT and Q67L expressing cells, indicated by arrows in the LC3 and merge columns. The centre of the rings typically showed labelling for Lamp1 as indicated by the arrows and inserts in the merge column. These structures were not observed in cells expressing GFP-Rab7 T22N. Bar, 20 μm.

increased LC3II after 2 hours starvation followed by 2 hours chase.

Although by electron microscopy we observed significantly more autophagic vacuoles in the RNAi cells (Fig. 6B), the levels of LC3II were only slightly or not at all affected in the Rab7 RNAi cells (Fig. 6A). In agreement with the LC3 western blotting, we did not observe grossly increased LC3 staining in immunofluorescence labelling of the Rab7 RNAi cells (Fig. 5C). This is probably due to the fact that LC3II levels are less affected in cells accumulating late autophagic vacuoles (Eskelinen et al., 2004), as opposed to cells accumulating more early autophagosomes (Kabeya et al., 2000). This is also in agreement with the immunoelectron microscopy of LC3, showing lower labelling density in AVd than in AVi.

To get more insight on the effect of Rab7 on autophagy, we also estimated the size of the autophagic vacuole profiles. The sizes of early and late autophagic vacuole profiles were similar in pSUPER and Rab7 RNAi cells: Avi, 0.39+0.04 μm^2 and 0.45+0.05 μm^2 in pSUPER and Rab7 RNAi cells, respectively (P=0.37, t-test); and Avd, 0.37 + 0.08 μm^2 and 0.33 + 0.06 μm^2 in pSUPER and Rab7 RNAi cells, respectively (P=0.71). These results further indicated that the initial maturation/fusion steps leading to the formation of morphologically identifiable late autophagic vacuoles were not affected by the deficiency of Rab7. Thus, we concluded that Rab7 had a role in the maturation of late autophagic vacuoles, possibly in the fusion with lysosomes.

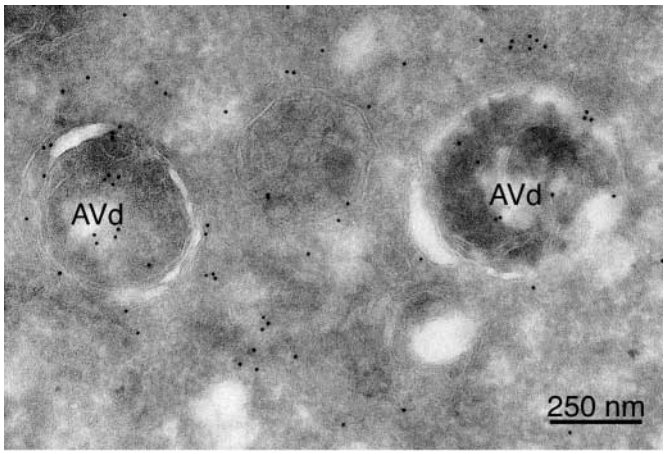

Fig. 8. Late autophagic vacuoles were observed in cells expressing GFP-Rab7 T22N. HeLa cells were transfected with GFP-Rab7 T22N. One day later the cells were starved of amino acids for 2 hours and prepared for immunogold labelling with anti-GFP and 10 nm gold-coupled secondary antibodies. Cells expressing GFP-Rab7 T22N accumulated late autophagic vacuoles (AVd).

Dominant negative Rab7 inhibited the formation of large LC3 structures and the maturation of late autophagic vacuoles

Overexpression of the T22N mutant of Rab7 has been used to inhibit the function of endogenous Rab7 (Bucci et al., 2000). We therefore analysed the effects of Rab7 wild type, constitutively active (Q67L) and the dominant negative (T22N) GFP-tagged constructs on LC3 distribution. HeLa cells were transiently transfected with one of the three constructs, cultured overnight and starved of amino acids for 2 hours. LC3 and Lamp1 were localised by immunofluorescence staining. In cells expressing wild-type Rab7, the LC3 localisation was similar to nontransfected cells after 2 hours starvation (see Fig. 1, Fig. 5A,B); both small scattered vesicles and large ring-like mainly perinuclear LC3 structures were seen (Fig. 7, upper row). Similar to earlier results (Fig. 5B), Lamp1 staining was observed inside the LC3-positive ring-shaped structures (Fig. 7, merged image in the upper row). A similar LC3 pattern was seen in cells expressing Rab7 Q67L, but the number of the large LC3/Lamp1-positive structures was slightly higher (Fig. 7, middle row). Quantitation showed that 35% of cells expressing wild-type Rab7 and 40% of cells expressing Rab7 Q67L contained large LC3/Lamp1-positive structures. On the contrary, only 5% of cells expressing the dominant negative Rab7 T22N showed large LC3/Lamp1-positive structures. In these cells only the small LC3 vesicles were observed (Fig. 7, lower row), in agreement with the Rab7 RNAi cells (Fig. 5C). Some colocalisation of LC3 and Lamp1 was observed in these small vesicles, which is in agreement with the finding that autophagosomes were able to mature into late autophagic vacuoles in the absence of functional Rab7 (Fig. 6B). Unexpectedly, the proportion of cells showing large perinuclear LC3 structures was around 70% in nontransfected cells (Fig. 1) or cells transfected with the empty pSUPER (Fig. 5A), but only 35% in cells overexpressing wild-type Rab7 (Fig. 7). Thus, it seemed that rather than inducing the large LC3 structures, overexpression of Rab7 inhibited their formation. It is possible that overexpression of Rab7 sequestered some effectors, such as GDI and REP (Somsel Rodman and Wandinger-Ness, 2000; Stenmark and Olkkonen, 2001), shared by other Rab proteins, which may also be necessary for autophagic vacuole maturation. In any case, the proportion of cells containing ring-like LC3-positive structures was significantly higher in cells expressing wild-type or constitutively active Rab7 (35-40%) than in those expressing the dominant negative Rab7 (5%).

We also investigated the autophagic vacuole maturation by electron microscopy. Similar to the Rab7 RNAi cells (Fig. 6B), late autophagic vacuoles were observed in cells expressing GFP-Rab7 T22N (Fig. 8), indicating that the conversion of AVi into AVd was not prevented by inactivation of Rab7.

Taken together, these results suggested that the overexpression of the dominant negative Rab7 T22N construct inhibited the formation of the large, mainly perinuclear LC3/Lamp1-positive structures but did not prevent the initial maturation of early autophagic vacuoles into late autophagic vacuoles. This confirmed our findings with Rab7 RNAi (see Figs 5, 6).

Recruitment of Rab7 to autophagic vacuoles was retarded in cells deficient in Lamp1 and Lamp2

We recently reported that large amounts of late autophagic vacuoles accumulated during starvation in mouse embryonic fibroblasts (MEFs) deficient in Lamp1 and Lamp2 (Eskelinen et al., 2004). Similar to cells treated with Rab7 RNAi, in the Lamp double deficient cells the amount of early autophagic vacuoles was similar to wild-type cells, whereas the amount of late vacuoles was more than twice as high as in the wild-type cells. Also identical with the Rab7 RNAi cells, LC3II levels in the Lamp-deficient cells were only mildly affected. The Lamp double deficient cells also accumulated large amounts of unesterified cholesterol in their endo/lysosomal compartment (Eskelinen et al., 2004). Cholesterol accumulation has been shown to inhibit Rab7 membrane extraction by the guanine nucleotide dissociation inhibitor and thus to increase the amount of membrane-associated Rab7 (Lebrand et al., 2002), which was shown to interfere with Rab7 function. In accordance with this, we observed increased vesicular staining of endogenous Rab7 and transfected GFP-Rab7 in the Lamp double deficient cells by immunofluorescence microscopy (Eskelinen et al., 2004). These findings raised the question whether the lack of functional Rab7 would be the cause of late autophagic vacuole accumulation in Lamp1 and Lamp2 deficient MEFs. To test this we investigated the recruitment of Rab7 to autophagic vacuoles. Wild-type control and Lamp1/Lamp2 deficient MEFs were transiently transfected with GFP-Rab7. The next day the cells were starved of serum and amino acids for 1 or 2 hours, fixed and prepared for immunofluorescence staining with LC3 antibodies. Colocalisation of GFP-Rab7 and LC3 was quantitated. Significantly less recruitment of Rab7 to LC3-positive vesicles was observed in Lamp1/Lamp2 deficient cells when compared with the control cells (Fig. 9A,B). In addition, in control cells the LC3-positive vesicles were often observed in the perinuclear region (Fig. 9A, red and yellow), whereas in Lamp1/Lamp2 deficient cells they were more scattered around the cytoplasm a long way from the nucleus (Fig. 9B, red and

yellow). These findings suggested that the recruitment of Rab7 to autophagic vacuoles was retarded in MEFs deficient in Lamp1 and Lamp2. The lack of Rab7 was the probable cause for the retarded accumulation of autophagic vacuoles in the perinuclear region (Fig. 9A,B), and for the retarded maturation of late autophagic vacuoles as detected by electron microscopy (Eskelinen et al., 2004). The Lamp double deficient cells thus represented an independent model with disturbed maturation of late autophagic vacuoles, probably caused by impaired Rab7 function.

Discussion

After the present paper had been submitted, Gutierrez et al. reported that Rab7 was required for the progression of autophagy in mammalian cells (Gutierrez et al., 2004). In agreement with our results, Gutierrez et al. showed that GFP-Rab7 localised in autophagic vacuoles. Further, they observed that in cells overexpressing the dominant negative Rab7 T22N, endosomes were still able to fuse with autophagic vacuoles. We also observed fusion of multivesicular endosomes with autophagic vacuoles in the Rab7 RNAi cells (not shown). Similar to us, Gutierrez et al. concluded that Rab7 was probably needed for fusion of autophagic vacuoles with lysosomes, which was probably necessary for the final degradation of the segregated cytoplasm.

In contrast to our electron microscopical data, showing that the size of autophagic vacuoles was similar in pSUPER and Rab7 RNAi cells, Gutierrez et al. (Gutierrez et al., 2004) reported that cells expressing the dominant negative Rab7 T22N accumulated larger autophagic vacuoles than cells expressing wild-type Rab7. In addition, Gutierrez et al. did not report the appearance of large, ring-shaped structures positive for LC3 and endo/lysosomal markers after longer starvation periods. These discrepancies could be due to one of the following reasons. First, Gutierrez et al. used cells with stable overexpression of GFP-Rab7 T22N. Continuous overexpression of dominant negative Rab7 was likely to cause defects in late endosomal/lysosomal biogenesis, given that Rab7 is known to have a role in this process (Bucci et al., 2000). Defects in late endosomal/lysosomal function in turn are likely to affect the autophagic process. In the present paper we used transient transfection of the Rab7 RNAi constructs or GFP-Rab7 T22N, which was less likely to cause major disturbances in lysosome biogenesis. Further, as discussed above, overexpression of one Rab protein may inhibit the functions of several other Rab proteins by sequestering effector proteins. This problem does not concern our Rab7 RNAi experiments. Overexpression of Rab7 might also explain why Gutierrez et al. did not see the large ring-shaped LC3 structures. We observed these structures frequently in normal cells, but less frequently in cells overexpressing Rab7 wild type, constitutively active or especially the dominant negative mutant. Second, Gutierrez et al. used overexpressed myc-tagged LC3, or the fluorescent compound monodansylcadaverine (MDC), to detect autophagic vacuoles. With overexpressed LC3 the authors were likely to detect more compartments, possibly including very advanced autophagic structures or even lysosomes. With endogenous LC3 or transmission electron microscopy, we were more likely to detect early and late autophagic vacuoles specifically. In addition, the same group has shown earlier that overexpression of LC3 induced autophagy (Munafo and Colombo, 2002). Our preliminary experiments suggested that overexpression of LC3 may cause increased recruitment of Rab7 to LC3-positive vesicles (not shown), and therefore we chose to use endogenous LC3. However, MDC is not a specific marker of autophagic vacuoles. Gutierrez et al. (Gutierrez et al., 2004) stated that it is acidotropic, meaning that it may stain all acidic compartments, including late endosomes and lysosomes. The specificity of MDC is further challenged by the results reported in Gutierrez et al. Using MDC, the authors reported that the number of autophagic vacuoles decreased in the Rab7 T22N-expressing cells. However, using overexpressed LC3, they reported that the autophagic vacuole number actually increased in these cells. The result with LC3 is in agreement with our

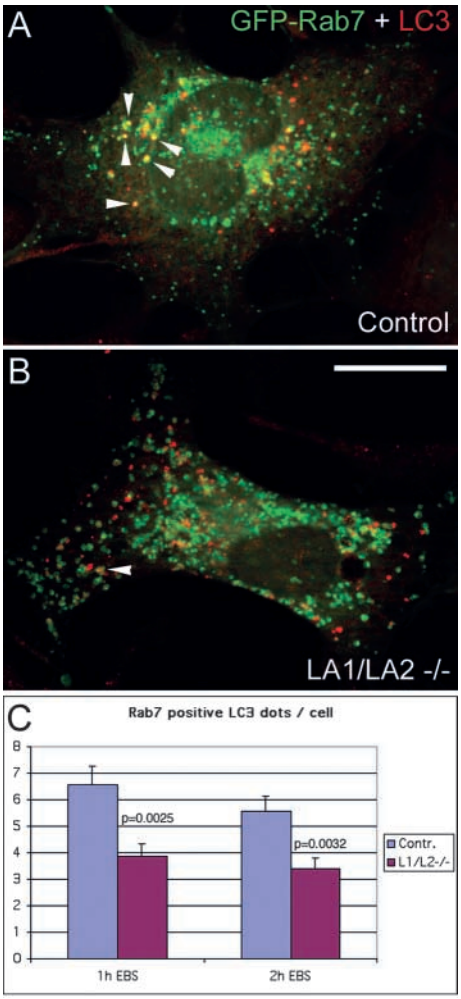

Fig. 9. Recruitment of Rab7 to autophagic vacuoles was retarded in mouse fibroblasts deficient in Lamp1 and Lamp2. Control (A) and Lamp1/Lamp2-deficient (B) cells were transiently transfected with GFP-Rab7 (green), grown for 1 day, and starved of serum and amino acids (EBS) for 1 hour (A, B) or 2 hours (not shown). The cells were fixed and prepared for immunofluorescence staining with anti-LC3 (red). Optical sections are shown. Colocalisation of LC3 and Rab7 (arrowheads) was quantitated as the number of yellow dots per cell (C). The *P* values indicate statistical significance compared to the control cells (*t*-test). Bar, 20 μm.

electron microscopical findings. Third, Gutierrez et al. used only light microscopy to estimate the size of the autophagic structures. This method has much lower resolution than transmission electron microscopy used in our study. Fourth, Gutierrez et al. used CHO cells and we used HeLa cells. It is possible, although less likely, that the maturation of autophagic vacuoles varies in different cell types.

Recruitment of Rab7 to phagosomes has been shown to precede and to be essential for phagosome fusion with endosomes and lysosomes (Harrison et al., 2003). In HeLa cells starved of amino acids to induce autophagy, we observed colocalisation of LC3 with Rab7 at very early time points, whereas colocalisation of LC3 with endo/lysosomal markers was observed later, suggesting that Rab7 was delivered to autophagosomes before fusion with endo/lysosomal vesicles. These findings suggest that Rab7 has a similar role in assisting the maturation of phagosomes and autophagic vacuoles. However, we observed accumulation of predominantly late autophagic vacuoles in cells expressing the Rab7 RNAi construct or the dominant negative Rab7. Thus it seems that Rab7 is not needed for the initial maturation steps, probably including fusion with endosomal vesicles, that convert autophagosomes to late autophagic vacuoles. This interpretation is in agreement with the results of Gutierrez et al. (Gutierrez et al., 2004). Rather, it seems that Rab7 has a role in the final maturation of late autophagic vacuoles, most probably in the fusion with lysosomes. It is also possible that Rab7 is needed for transport of degradation products out of late autophagic vacuoles. This is different from the yeast, where deletion of Ypt7 as good as completely blocked fusion of autophagosomes with the vacuole (Kirisako et al., 1999). It is likely that in yeast cells the maturation of autophagosomes is a simple one-step fusion with the vacuole, as only early autophagosomes, containing intact cytoplasm, accumulated in starved Ypt7-deficient cells (E. L. Eskelinen, unpublished).

Interestingly, we observed that LC3-positive autophagosomes formed at random locations around the cytoplasm. During longer starvation periods (2-4 hours), larger LC3-positive structures appeared mainly in the perinuclear region, suggesting that the small vesicles formed larger aggregates. By electron microscopy we observed that these aggregates typically located near the Golgi apparatus and consisted of several autophagic vacuoles surrounding a late endosomal/lysosomal vesicle, about to fuse with the latter to deliver their cargo for degradation. With increasing starvation time the small LC3-positive vesicles were reducing in number while the larger, mainly perinuclear LC3 structures appeared. Rab7 RNAi and dominant negative Rab7 inhibited the formation of the large LC3-positive structures. This suggests that fusion of autophagic vacuoles with the late endosomes/lysosomes located close to the Golgi apparatus is necessary for their final maturation and degradation of the segregated cytoplasmic contents. Phagosomes also move from the cell periphery to the perinuclear area, and this movement is mediated by the Rab7 effector protein RILP (Harrison et al., 2003). Thus it is possible that RILP also participates in autophagosome movements. Although the formation process of autophagosomes is completely different from phagosomes originating from the plasma membrane, it seems that there may be common features during the later steps of these two degradation pathways.

Microtubule inhibitors, which completely stop all microtubule-dependent transport, cause accumulation of mainly early (vinblastine) (Hirsimaki and Pilstrom, 1982) or intermediate autophagic vacuoles (nocodazole) (Aplin et al., 1992). The intermediate vacuoles would be classified as late autophagic vacuoles (Avd) in our quantitative electron microscopy. Thus the effect of Rab7 inhibition on autophagic vacuole accumulation resembles the effect of microtubule disruption by nocodazole. Vinblastine has been proposed to be less specific than nocodazole. It may also directly inhibit lysosomal degradation, which might explain its more drastic effect on autophagic vacuole maturation.

In this paper we showed that after their formation LC3-positive autophagic vacuoles accumulated in larger aggregates mainly in the perinuclear area and that Rab7 was needed for this event. We also showed that Rab7 localised in the limiting membranes of autophagic vacuoles and that it was delivered to them before the delivery of late endosomal/lysosomal proteins. Using quantitative electron microscopy we further showed that Rab7 was required for the final maturation of late autophagic vacuoles, possibly for fusion with lysosomes. Future experiments will show what kind of other Rab proteins and/or other fusion proteins are necessary for autophagic vacuole maturation in mammalian cells.

We thank Suzanne Pfeffer and Angela Wandinger-Ness for Rab7 antibodies, Jean Gruenberg for anti-LBPA and Bo van Deurs for GFP-Rab7 constructs. We are grateful to Marlies Rusch and Katharina Stiebeling for technical assistance. This work was supported by The Royal Society of London to E.L.E., the Deutsche Forschungsgemeinschaft, and Fonds der Chemischen Industrie to P.S.

References

Abeliovich, H., Dunn, W. A., Kim, J. and Klionsky, D. J. (2000). Dissection of autophagosome biogenesis into distinct nucleation and expansion steps. *J. Cell Biol.* **151**, 1025-1034.

Aplin, A., Jasionowski, T., Tuttle, D. L., Lenk, S. E. and Dunn, W. A. (1992). Cytoskeletal elements are required for the formation and maturation of autophagic vacuoles. *J. Cell. Physiol.* **152**, 458-466.

Arstila, A. U. and Trump, B. F. (1968). Studies on cellular autophagocytosis. The formation of autophagic vacuoles in the liver after glucagon administration. *Am. J. Pathol.* **53**, 687-733.

Atlashkin, V., Kreykenbohm, V., Eskelinen, E. L., Wenzel, D., Fayyazi, A. and Fischer von Mollard, G. (2003). Deletion of the SNARE vti1b in mice results in the loss of a single SNARE partner, syntaxin 8. *Mol. Cell. Biol.* **23**, 5198-5207.

Berg, T. O., Fengsrud, M., Stromhaug, P. E., Berg, T. and Seglen, P. O. (1998). Isolation and characterization of rat liver amphisomes. Evidence for fusion of autophagosomes with both early and late endosomes. *J. Biol. Chem.* **273**, 21883-21892.

Bottger, G., Nagelkerken, B. and van der Sluijs, P. (1996). Rab4 and Rab7 define distinct nonoverlapping endosomal compartments. *J. Biol. Chem.* **271**, 29191-29197.

Brummelkamp, T. R., Bernards, R. and Agami, R. (2002). A system for stable expression of short interfering RNAs in mammalian cells. *Science* **296**, 550-553.

Bucci, C., Thomsen, P., Nicoziani, P., McCarthy, J. and van Deurs, B. (2000). Rab7: a key to lysosome biogenesis. *Mol. Biol. Cell* **11**, 467-480.

Darsow, T., Rieder, S. E. and Emr, S. D. (1997). A multispecificity syntaxin homologue, Vam3p, essential for autophagic and biosynthetic protein transport to the vacuole. *J. Cell Biol.* **138**, 517-529.

Dunn, W. A. (1990). Studies on the mechanisms of autophagy: maturation of the autophagic vacuole. *J. Cell Biol.* **110**, 1935-1945.

Dunn, W. A. (1994). Autophagy and related mechanisms of lysosomal-mediated protein degradation. *Trends Cell Biol.* **4**, 139-143.

Eskelinen, E. L. (2004). Autophagy in mammalian cells. In *Lysosomes* (ed. P. Saftig). Landes Bioscience/Eurekah.com. (Epub ahead of print).

Eskelinen, E. L., Illert, A. L., Tanaka, Y., Blanz, J., von Figura, K. and Saftig, P. (2002a). Role of LAMP-2 in lysosome biogenesis and autophagy. *Mol. Biol. Cell* **13**, 3355-3368.

Eskelinen, E. L., Prescott, A. R., Cooper, J., Brachmann, S. M., Wang, L., Tang, X., Backer, J. M. and Lucocq, J. M. (2002b). Inhibition of autophagy in mitotic animal cells. *Traffic* **3**, 878-893.

Eskelinen, E. L., Tanaka, Y. and Saftig, P. (2003). At the acidic edge: emerging functions for lysosomal membrane proteins. *Trends Cell Biol.* **13**, 137-145.

Eskelinen, E. L., Schmidt, C., Neu, S., Willenborg, M., Fuertes, G., Salvador, N., Tanaka, Y., Lüllmann-Rauch, R., Hartmann, D., Heeren, J. et al. (2004). Disturbed cholesterol traffic but normal proteolytic function in LAMP-1/LAMP-2 double deficient fibroblasts. *Mol. Biol. Cell* **15**, 3132-3145.

Gordon, P. B., Hoyvik, H. and Seglen, P. O. (1992). Prelysosomal and lysosomal connections between autophagy and endocytosis. *Biochem. J.* **283**, 361-369.

Gutierrez, M. G., Munafo, D. B., Beron, W. and Colombo, M. I. (2004). Rab7 is required for the normal progression of the autophagic pathway in mammalian cells. *J. Cell Sci.* **117**, 2687-2697.

Harrison, R. E., Bucci, C., Vieira, O. V., Schroer, T. A. and Grinstein, S. (2003). Phagosomes fuse with late endosomes and/or lysosomes by extension of membrane protrusions along microtubules: role of Rab7 and RILP. *Mol. Cell. Biol.* **23**, 6494-6506.

Hirsimaki, P. and Pilström, L. (1982). Studies on vinblastine-induced autophagocytosis in mouse liver. III. A quantitative study. *Virchows Arch. B Cell Pathol.* **41**, 51-66.

Ishihara, N., Hamasaki, M., Yokota, S., Suzuki, K., Kamada, Y., Kihara, A., Yoshimori, T., Noda, T. and Ohsumi, Y. (2001). Autophagosome requires specific early Sec proteins for its formation and NSF/SNARE for vacuolar fusion. *Mol. Biol. Cell* **12**, 3690-3702.

Kabeya, Y., Mizushima, N., Ueno, T., Yamamoto, A., Kirisako, T., Noda, T., Kominami, E., Ohsumi, Y. and Yoshimori, T. (2000). LC3, a mammalian homologue of yeast Apg8p, is localized in autophagosome membranes after processing. *EMBO J.* **19**, 5720-5728.

Kirisako, T., Baba, M., Ishihara, N., Miyazawa, K., Ohsumi, M., Yoshimori, T., Noda, T. and Ohsumi, Y. (1999). Formation process of autophagosome is traced with Apg8/Aut7 in yeast. *J. Cell Biol.* **147**, 435-446.

Klionsky, D. J. and Emr, S. D. (2000). Autophagy as a regulated pathway of cellular degradation. *Science* **290**, 1717-1721.

Kobayashi, T., Stang, E., Fang, K. S., de Moerloose, P., Parton, R. G. and Gruenberg, J. (1998). A lipid associated with the antiphospholipid syndrome regulates endosome structure and function. *Nature* **392**, 193-197.

Lang, T., Schaeffeler, E., Bernreuther, D., Bredschneider, M., Wolf, D. H. and Thumm, M. (1998). Aut2p and Aut7p, two novel microtubule-associated proteins are essential for delivery of autophagic vesicles to the vacuole. *EMBO J.* **17**, 3597-3607.

Lawrence, B. P. and Brown, W. J. (1992). Autophagic vacuoles rapidly fuse with pre-existing lysosomes in cultured hepatocytes. *J. Cell Sci.* **102**, 515-526.

Lebrand, C., Corti, M., Goodson, H., Cosson, P., Cavalli, V., Mayran, N., Faure, J. and Gruenberg, J. (2002). Late endosome motility depends on lipids via the small GTPase Rab7. *EMBO J.* **21**, 1289-1300.

Liang, X. H., Jackson, S., Seaman, M., Brown, K., Kempkes, B., Hibshoosh, H. and Levine, B. (1999). Induction of autophagy and inhibition of tumorigenesis by beclin 1. *Nature* **402**, 672-676.

Liou, W., Geuze, H. J., Geelen, M. J. H. and Slot, J. W. (1997). The autophagic and endocytic pathways converge at the nascent autophagic vacuole. *J. Cell Biol.* **136**, 61-70.

Lucocq, J. and Walker, D. (1997). Evidence for fusion between multilamellar endosomes and autophagosomes in HeLa cells. *Eur. J. Cell Biol.* **72**, 307-313.

Melendez, A., Talloczy, Z., Seaman, M., Eskelinen, E. L., Hall, D. H. and Levine, B. (2003). Autophagy genes are essential for dauer development and lifespan extension in C. elegans. *Science* **301**, 1387-1391.

Mizushima, N., Ohsumi, Y. and Yoshimori, T. (2002). Autophagosome formation in mammalian cells. *Cell Struct. Funct.* **27**, 421-429.

Möbius, W., van Donselaar, E., Ohno-Iwashita, Y., Shimada, Y., Heijnen, H. F. G., Slot, J. W. and Geuze, H. J. (2003). Recycling compartments and the internal vesicles of multivesicular bodies harbor most of the cholesterol found in the endocytic pathway. *Traffic* **4**, 222-231.

Munafo, D. B. and Colombo, M. I. (2002). Induction of autophagy causes dramatic changes in the subcellular distribution of GFP-Rab24. *Traffic* **3**, 472-482.

Nara, A., Mizushima, N., Yamamoto, A., Kabeya, Y., Ohsumi, Y. and Yoshimori, T. (2002). SKD1 AAA ATPare-deficient endosomal transport is involved in autolysosome formation. *Cell Struct. Funct.* **27**, 29-37.

Press, B., Feng, Y., Hoflack, B. and Wandinger-Ness, A. (1998). Mutant Rab7 causes the accumulation of cathepsin D and cation-independent mannose 6-phosphate receptor in an early endocytic compartment. *J. Cell Biol.* **140**, 1075-1089.

Punnonen, E. L., Autio, S., Kaija, H. and Reunanen, H. (1993). Autophagic vacuoles fuse with the prelysosomal compartment in cultured rat fibroblasts. *Eur. J. Cell Biol.* **61**, 54-66.

Somsel Rodman, J. and Wandinger-Ness, A. (2000). Rab GTPases coordinate endocytosis. *J. Cell Sci.* **113**, 183-192.

Stenmark, H. and Olkkonen, V. M. (2001). The Rab GTPase family. *Genome Biol.* **2**, REVIEWS3007, Epub 2001 Apr 27.

Tanaka, Y., Guhde, G., Suter, A., Eskelinen, E. L., Hartmann, D., Lüllmann-Rauch, R., Janssen, P. M. L., Blanz, J., von Figura, K. and Saftig, P. (2000). Accumulation of autophagic vacuoles and cardiomyopathy in LAMP-2-deficient mice. *Nature* **406**, 902-906.

Tooze, J., Hollinshead, M., Ludwig, T., Howell, K., Hoflack, B. and Kern, H. (1990). In exocrine pancreas, the basolateral endocytic pathway converges with the autophagic pathway immediately after the early endosome. *J. Cell Biol.* **111**, 329-345.

Ueno, T., Muno, D. and Kominami, E. (1991). Membrane markers of endoplasmic reticulum preserved in autophagic vacuolar membranes isolated from leupeptin-administered rat liver. *J. Biol. Chem.* **266**, 18995-18999.

Vitelli, R., Santillo, M., Lattero, D., Chiariello, M., Bifulco, M., Bruni, C. B. and Bucci, C. (1997). Role of the small GTPase Rab7 in the late endocytic pathway. *J. Biol. Chem.* **272**, 4391-4397.